Journal of Materials Chemistry A

Accepted Manuscript

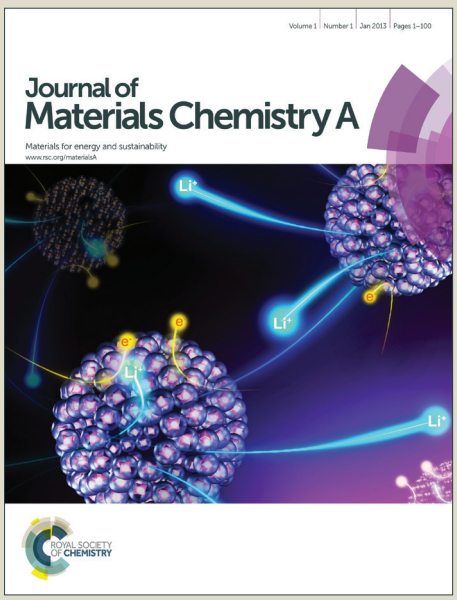

ROYAL SOCIETY OF CHEMISTRY

www.rsc.org/materialsA

Journal Name

RSCPublishing

ARTICLE

Controllable wettability and adhesion on bioinspired multifunctional TiO_2 nanostructure surfaces for liquid manipulation

Cite this: DOI: 10.1039/xoxxoooooox

Jianying Huang,[a] Yuekun Lai,*[a,b] Luning Wang,[c] Shuhui Li,[a] Mingzheng Ge,[a] Keqin Zhang,[a] Harald Fuchs[b] and Lifeng Chi[b,d]

Received ooth January 2012,
Accepted ooth January 2012

DOI: 10.1039/xoxxoooooox

www.rsc.org/

Hierarchical surfaces with specific topographical morphology and chemical component can be found on many living creatures in nature. They offer special wettability and adhesion (sliding, sticky or patterned superhydrophobic surfaces) a functional platform for microfluidic management and other biological functions. Inspired by their precise arrangement of structures and surface components, we described a facile one-step electrochemical technique to large scale create a dual-scale hierarchical anatase TiO_2 structures with the combination of pinecone-like micro-particle upper layer and dense-stacked nanoparticle bottom layer. The as-prepared TiO_2 films display environment-responsive wettability with good dynamical stability. Extremely high contrast of adhesion (2.5-170 μN) can be realized by simply adjusting the physical structures (anodizing voltage and electrolyte concentration dependent) to control the solid-liquid contact state (from "Rose" to "Lotus" state). In addition, erasable and rewritable patterned superhydrophobic TiO_2 films were constructed for a versatile platform for microfluidic management. In a proof-of-concept study, robust super-antiwetting films for on-demand droplet separation, mixing and transportation under ambient atmosphere or underwater environment, and patterned superhydrophobic surfaces for liquid self-assembling or anti-counterfeiting mark were demonstrated.

Introduction

Natural creatures with fascinating superwettability contain amazing hierarchical structure and chemical component arrangement, which inspire scientific researchers for solving many of mankind's greatest challenges.[1-3] There are some typical super-antiwetting cases in nature, such as low-adhesive superhydrophobic surfaces (lotus leaf & water strider leg),[4] high-adhesive superhydrophobic surfaces (rose petal & peanut leaf),[5] underwater superoleophobic surfaces (hark skin & fish scale),[6] and patterned superhydrophobic beetle's back with highly hydrophilic/phobic units.[7] Bioinspired TiO_2 hierarchical surfaces with extremely high contrast of wettability and adhesion property for water/oil contact angle (CA) above 150° or below 5°, have attracted extensive interest during recent years because of their fundamental science and practical industrial applications, such as self-cleaning,[8,9] droplet manipulation,[10,11] wetting template,[12,13] anti-bioadhesion,[14,15] and microfluidic devices.[16,17] For many of these applications, multifunctional surfaces with combined special water/oil wettability/adhesion in air or underwater environment, or highly wetting contrast patterning substrates are required for reliable manipulation or precise self-assembling expensive biofluids and reagents. Various synthesis techniques had been applied to fabricate multifunctional TiO_2-based hierarchical structures, such as hydrothermal method, template assisted deposition, and anodic oxidation coating have been investigated so far.[18,19] Several approaches have been developed to construct such TiO_2 surfaces with special wettability and adhesion, e.g. superhydrophobic surface with structures/chemical composition-induced tunable adhesion, stimuli-responsive switchable adhesion and patterned superwettability.[20,21] We reported the fabrication of TiO_2 structures by anodization approach followed by the perfluorosilane modification. The water droplet can be adjusted between sliding and sticky state on various superhydrophobic TiO_2 surfaces with specific structure, high energy materials introduction or masked UV irradiation.[22]

Electrochemical anodizing TiO_2 nanostructures have become a focus of tremendous interests due to its controllable rough structures and excellent photocatalytic activity to conveniently adjust surface chemical composition.[23,24] Therefore, the resultant wettability and adhesion on TiO_2 surface can be greatly influenced by UV illumination and amplified by the rough nanostructures. In this work, we applied a simple one-step and practical electrochemical anodizing approach to fabricate large scale pinecone-like anatase TiO_2 particles film. The as-prepared environment-responsive TiO_2 film exhibits superhydrophilic property in air, and changes to robust underwater superoleophobicity. The combined superhydrophobicity in air and superoleophilicity underwater with good dynamic stability can be achieved by a hydrogen-bond-driven process for *1H, 1H, 2H, 2H*-perfluorodecyltriethoxysilane (PDES) assembling. The results showed that the TiO_2 surfaces prepared by an anodizing voltage of

50 V with an NH_4F concentration of 0.01-0.05 M have a dual-scale hierarchical structure, and exhibited the best super-antiwetting performance (high contact angle & low adhesion) and crystallization state of anatase phase. This suggests that the topography of the anatase TiO_2 structures plays important role on special wettability and adhesion. Additionally, erasable and rewritable patterned superhydrophobic TiO_2 film with extreme wettability contrast (superhydrophilic/superhydrophobic) can be constructed by alternating photocatalytic lithography and monolayer self-assembly. The hierarchical anatase TiO_2 particle surfaces with robust superwetting/antiwetting properties would be a versatile platform in a wide range of applications, especial for microfluidic management (e.g., micro-droplets manipulation, liquid self-assembling, and miniature reactor). In a proof-of-concept study, we investigated super-antiwetting films for on-demand droplet separation, mixing and transportation in air or underwater environment, and patterned superhydrophobic surfaces for liquid self-assembling or anti-counterfeiting mark.

Experimental section

Preparation of anti-wetting TiO_2 Surface: Titanium sheets with a thickness of 0.127 mm and a purity of 99.7% were purchased from Sigma-Aldrich. The superhydrophobic anatase TiO_2 particle films were prepared by a combination of electrochemically anodizing and self-assembly monolayer technique. Firstly, titanium sheets were anodized in 0.01 M NH_4F electrolyte at 50 V for a certain time with a Pt counter electrode (this concentration and voltage will be used in subsequent experiments unless mentioned otherwise). The superhydrophobic surfaces were obtained by soaking the as-prepared anatase TiO_2 film in a mixed methanolic solution of hydrolyzed 1 v% of 1H, 1H, 2H, 2H-perfluorodecyltriethoxysilane (PDES) for 1 h and subsequently baked at 140 ^oC for 1 h.

Characterization of TiO_2 Structure Film: The surface structure was examined by a Hitachi S-4800 field-emission scanning electron microscope at 3.0 kV. The chemical compositions were studied by X-ray photoelectron spectroscopy (XPS, VG ESCALAB MK II) using a 300 W Al Ka X-ray source (1486.6 eV photons) with a base pressure about 3×10^{-9} mbar. The crystallinity of the as-prepared samples was measured using an X-ray diffractometer with $Cu_{K\alpha}$ radiation (XRD, Phillips X'pert-PRO PW3040). Deionized water was employed as the source for the CA measurement. The wetting properties of water droplets on the sample surfaces were characterized using an optical contact-angle meter system (Krüss DSA 100, Germany). The volume of droplet used for the static contact angle and dynamic sliding angle measurement was 10 μL. The adhesive force was measured using a high-sensitivity micro-electromechanical balance system (Dataphysics DCAT11, Germany). Water droplets of 4 μL suspending on a hydrophobic metal ring were approached and retracted from the sample surface at a constant speed of 0.01mm s^{-1} at ambient environment with relative humidity about 50%. The droplet started to move away from the sample surface once the equipment detected a force of 0.01 mg. Subsequently, the balance force would gradually increase, and reached the maximum before the droplet broke away from the surface. The peak data recorded in the force-distance curve was taken as the maximum adhesive force. The values reported were the average of five drops at different locations.

Results and discussion

Figure 1a-c shows the typical top-view SEM images of the as-anodized TiO_2 particles nanocomposite film with a double-layer hierarchical structure. It is seen that the upper layer has uniformly-distributed pinecone-like TiO_2 microscale protrusions with radial multilayer nanosheets grew out on Ti substrate to form fractal structure, the bottom diameter and height of the vertically orientated pinecone-like TiO_2 protrusions is approximately 3.0 and 5.0 μm, respectively. Apart from pinecone-like microparticles, a cross-stacked TiO_2 nanoparticle bottom layer appeared dense and compact (Fig. 1b). Water rapidly spreads and wets this as-anodized TiO_2 film due to side penetration of the liquid by capillary forces, indicating such sample is superhydrophilic (inset of Figure 1b), and changes to robust underwater superoleophobicity (Movie S1). Therefore, such environment-responsive TiO_2 film can be potentially acted as underwater robot fixed and working at the oil/water interface. However, it is observed that the droplets with spherical shapes slide spontaneously and hardly come to rest even when it is placed gently on the *1H, 1H, 2H, 2H*-perfluorooctyltriethoxysilane (PDES) modified TiO_2 surface. The intrinsic water CA on such super-antiwetting film is as high as 167°. Figure 2a displayed the effect of UV light irradiation on contact angle of photo-responsive TiO_2 nanostructure surfaces. By taking advantage of the excellent photocatalytic activity of the one-step as-prepared crystallized TiO_2 film and the amplification effect of rough hierarchical structure, the superhydrophobic surface quickly changed to superhydrophilic surface by UV irradiation within 30 min to photodegradate the low surface energy PDES monolayer. This suggests that reversible extreme or controllable wettability can be achieved by PDES modification and UV irradiation to alter the chemical component on photo responsive TiO_2 surface (Figure 1d).

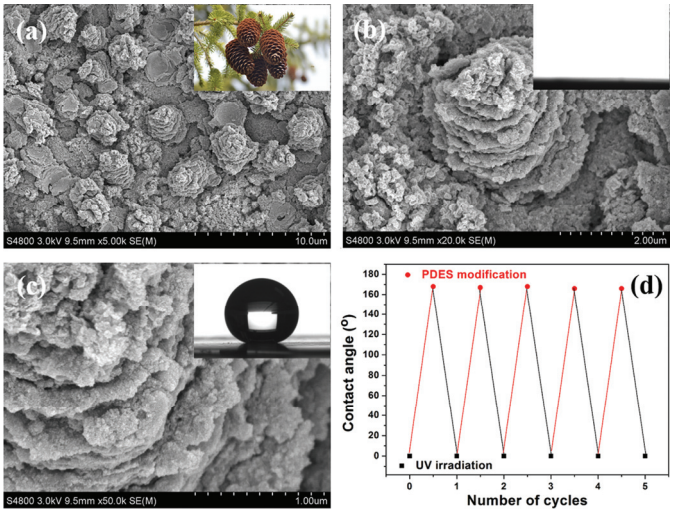

Figure 1. Typical top-view SEM (a-c) images of the as-anodized hierarchical pinecone-like structure TiO_2 film by electrochemical anodizing in 0.01 M NH_4F solution (50 V for 60 min). (d) Reversible surface wettability on TiO_2 film by alternating PDES modification and UV irradiation. The inset of (a) shows the photo image of pinecones on pine tree. The insets of figure 1b,c show the optical image of a water droplet on the as-prepared and PDES modified TiO_2 surface.

X-ray photoelectron spectroscope (XPS) was used to confirm the surface component change of the TiO_2 surface after PDES modification and UV irradiation. The results demonstrate the

existence of element Ti, O, C, F and Si on the surface (Fig. 2b). The presence of the strong F 1s peak and C 1s peak (due to C-F), together with the Si 2p appearance and attenuation of the Ti 2p and Ti 2s peaks confirm that PDES has been successfully self-assembled onto the pinecone-like TiO_2 surface (Fig. 2a,b). Another obvious character of the presence of PDES monolayer is the large intensity increase of the F 1s peak at 689.0 eV and the sharp intensity decrease of the F 1s at 684.4 eV (Fig. 2d). The main peak corresponding to CF_x indicates that the PDES coating on the outermost surface while the metal fluoride peak at 684.4 eV is ascribed to the anion uptake into the oxide layers during the anodizing process in fluoride containing solution. However, when UV light irradiate the PDES modified TiO_2 film, the F 1s peak at 689.0 eV is greatly weakened (Fig. 2d) while a stronger C-H peak at 284.8 eV appears (Fig. 2c). Therefore, it is reasonable to conclude that the low surface energy fluorocarbon group has been degraded by the photocatalytic activity of TiO_2 film under UV light illumination. Such surface chemical component change play vital role for the wettability response of the corresponding surfaces.

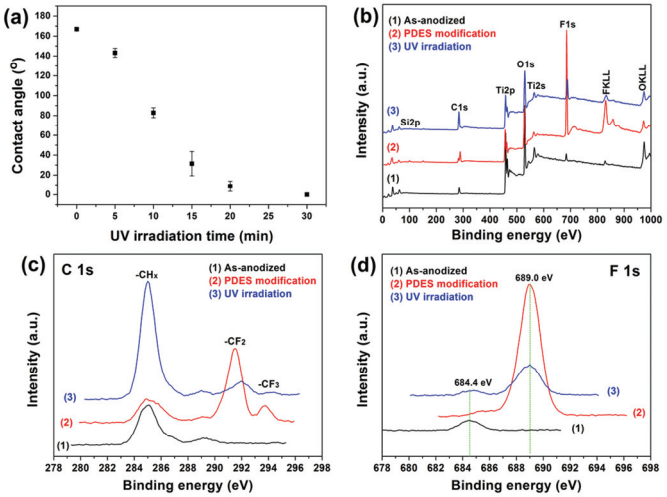

Figure 2. (a) The effect of UV light irradiation on contact angle of photo-responsive TiO_2 nanostructure surfaces. XPS survey (b) and high-resolution C1s (c) and F1s (d) spectra of TiO_2 surface before (1), after PDES modification (2) and following UV irradiation (3).

In order to investigate the influence of anodizing voltage and NH_4F concentration on the surface morphology, a set of experiments was systematically performed. It is found that the applied voltage, concentration of NH_4F have a great effect on the structure of TiO_2 film. Figure 3 shows FESEM image of the as-prepared TiO_2 structures obtained at different anodizing voltages (i.e., from 10 to 60 V) in 0.01 M NH_4F solution for 1 h. At low anodizing voltage (10, 20 V; Fig. 3a,b), nearly nanoparticle and nanopore structures formed. As the voltage increased to 40 V (Fig. 3c), pinecone-like microscale particles started to appear on nanostructure surface. As the voltage increased from 40 to 50 V (Fig. 1a-c), the amount of pinecone-like particles and their size increased resulted in the formation of a hierarchical dual-scale structure. When the applied voltage was further increased to 60 V (Fig. 3d), no obvious changes in the size of particles could be observed, while the density of pinecone-like particles and the mechanical strength of the as-prepared film decreased resulted from the rapid electrochemical reaction.

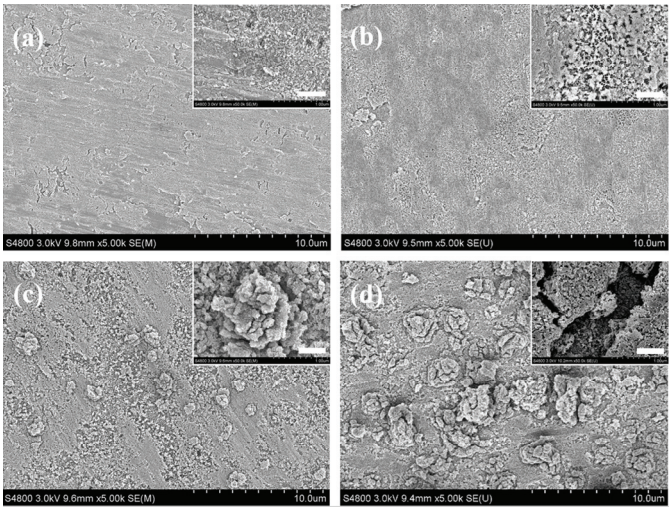

Figure 3. FESEM images showing the as-prepared structured TiO_2 when the Ti foil was anodized in 0.01M NH_4F solution for 1 h under various voltages: (a) 10 V; (b) 20 V; (c) 40 V; and (d) 60 V. The scale bar in inset is 500 nm

Figures 4 shows FESEM images of the as-prepared structured TiO_2 when the Ti foils are anodized with a constant potential of 50 V for 1 h in various NH_4F concentrations. At low concentration of NH_4F (0.005 M; Fig. 4a), only compact and cross-stacked nanoparticles structure are formed. As the concentration increased to 0.01 M (Fig. 4b), pinecone-like microscale particles started to appear on nanostructure surface to form a hierarchical micro-nano dual-scale composite structure. As the concentration increased from 0.01 to 0.05 M (Fig. 4c), no obvious changes in the amount and the size of particles of pinecone-like particles could be observed. When the concentration was further increased (Fig. 4d,e), obvious changes in the size, density and morphology of the top layer of microscale particles could be observed. The pinecone-like microscale particle with stacked plate-like nanoscale sheets change to random aggregated nanoparticles (inset of Fig. 4d), and the particles density and size obviously decreased. Consequently, a film with uniform nanoporous structure is formed with the disappearance of upper microscale particles (Fig. 4f). As a result, novel pinecone-like TiO_2 film with hierarchical structures can only be obtained under certain parameter (voltage: 40-60 V; concentration: 0.01-0.05 M).

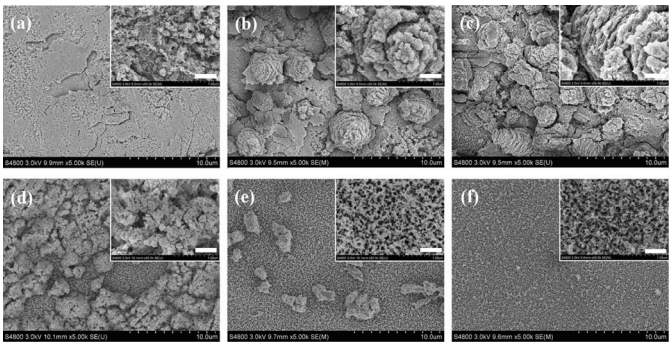

Figure 4. FESEM images showing the as-prepared structured TiO_2 when the Ti foil was anodized with a constant potential of 50 V for 1 h in various concentration of NH_4F solution: (a) 0.005 M; (b): 0.01 M; (c): 0.05 M; (d): 0.1 M; (e) 0.2 M; and (f) 0.5 M. The scale bar in inset is 500 nm

The one-step as-prepared crystallization assumption is also verified by the XRD result in Figure 5. Except the Ti substrate peaks, four broad diffraction peaks at 2θ = 25.4, 37.8, 48.0, 54.5° can be indexed to anatase phase TiO_2 of (101), (004), (200), and (105) planes, respectively (JCPDS No. 21-1272). The current work proves that crystalline anatase TiO_2 can be directly fabricated by a facile one-step electrochemical anodizing process in an environmentally-friendly electrolyte without the assistance of annealing process. During experiment, it was observed that the electrolyte temperature increased to some extent (approx. 40-60°C) with the increase of anodizing voltage (40-60 V) for 1 h due to the exothermic heat caused by the vigorous electrochemical process. The resultant TiO_2 composite structure becomes rougher as the electrochemical anodizing voltage enhances. The increased electrolyte temperature provides a greater driving force for ionic conduction and enhances the crystalline phase formation. Moreover, the intensity of the anatase crystal phase increased with the concentration increased to 0.05 M (Fig. 5b). This is highly related the amount and size of pinecone-like anatase TiO_2 particles formation on the upper layer of the composite film. Further increase the electrolyte concentration, the rigorous electrochemical etching process resulted in the detachment of pinecone-like anatase TiO_2 particles and the exposure of nanoparticles or even porous bottom TiO_2 layer (Fig. 4d-f). Therefore, we attribute the crystallization of the amorphous TiO_2 nanostructures to the dissolution and recrystallization mechanism. Similar results on the special role of the water in the transformation from amorphous TiO_2 to anatase TiO_2 at low temperature were also reported,[25] which only occurred during the sol-gel processes. This is different from the amorphous TiO_2 nanotube structure anodized in harmful HF solution, which requires further annealing post-treatment (above 300 °C) to form crystalline anatase phase.[26]

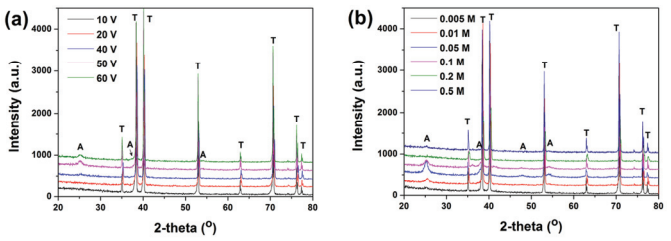

Figure 5. (a) XRD patterns of TiO_2 nanostructure layers anodized in 0.01 M NH_4F electrolyte for 1 h under various voltages; (b) XRD patterns of TiO_2 nanostructure layers anodized at 50 V for 1 h in various electrolyte concentrations, where the peaks representing anatase and the Ti substrate are labelled A and T, respectively.

Except the influence of surface morphology and the crystalline phase, the anodizing voltage and NH_4F concentration also have a great effect on static and dynamic wetting behaviour (Fig. 6a,b) and adhesion (Fig. 6c,d). Although all the PDES modified TiO_2 surfaces have the similar high hydrophobicity or even superhydrophobicity in air, the dynamic behavior and adhesion property are rather different on the surface. When the anodizing voltage was less than 10 V or concentration was lower than 0.01 M, droplets are not easily roll off the high-adhesive TiO_2 nanoparticle structure surface even when the substrate is vertically tilted. The adhesive force on 10 V anodized surface is highly about 170 μN measured by using a high-sensitivity micro-electromechanical balance. Such superhydrophobic nanoparticle structure exhibited a typical "Rose" liquid-solid state with ''area-contact'' behavior and continuous three-phase (solid-air-liquid) contact line (Fig. 7a). Moreover, negative pressure caused by the volume change of air sealed in the closed nanopore units may also play an important role for such ultra-high adhesive force. Increasing the anodizing voltage to 20 V, the static contact angle greatly increases to about 147°, but the droplet still firmly adhered on the surface with a sliding angle (SA) approx. 40°. Further increasing the voltage (40-60 V), the contact angle slightly increases to approach a platform of 168°, while the sliding angle drastically decrease to below 5° exhibiting a super-antiwetting state with a rare liquid adhesion of 2.5 μN (50 V). Up to now, only limited information on such ultralow adhesion phenomenon has been reported. This is ascribed to the typical point-contact model for greatly decrease of liquid-solid area, and the high ratio of air trapped into the hierarchical structures to form extremely discrete three-phase (solid-air-liquid) contact line.[22a] For anodized with various electrolyte concentrations, all the TiO_2 structures displayed static superhydrophobic property (Fig. 6b). However, the qualitative dynamic behaviour and quantitative adhesive force changes greatly. Except the high-adhesive surface with a SA of about 45° prepared by an electrolyte of 0.005 M NH_4F, all others displayed low-adhesion ability with a SA lower than 5°. For the sample anodized in 0.1 M NH_4F, it is verified with an unusual high adhesion about 25 μN (Fig. 4d), which is probably ascribed to the replacement of hierarchical composite structure of pinecone-like microparticle with stacked plate-like nanoscale sheets to random aggregated nanoparticle structure. Such structure conversion resulted in a higher contact area and continuous three-phase line than pine-cone like (Fig. 4b,c) hierarchical or nanoporous (Fig. 4e,f) structure.[22a] A more uniform nanoporous structure films were obtained with the increase of electrolyte concentration to 0.5 M. This was ascribed to the stronger electric field induced etching of TiO_2 film in high concentrated NH_4F electrolyte. Compared to high-adhesive nanoparticle structure (voltage: 10-20 V; concentration: 0.005 M, Fig. 7a) and hierarchical structure with ultra-low adhesion (voltage: 50-60 V; concentration: 0.01-0.05 M, Fig. 7b), such nanoporous structure surface exhibited a medium adhesion (voltage: 50 V; concentration: 0.1-0.5 M, Fig. 7c). Consequently, these results indicate that we can construct both low- and high-adhesion anti-wetting surface with mimicking lotus leaf and rose petal effects by simply adjusting the surface structure without changing the chemical component.

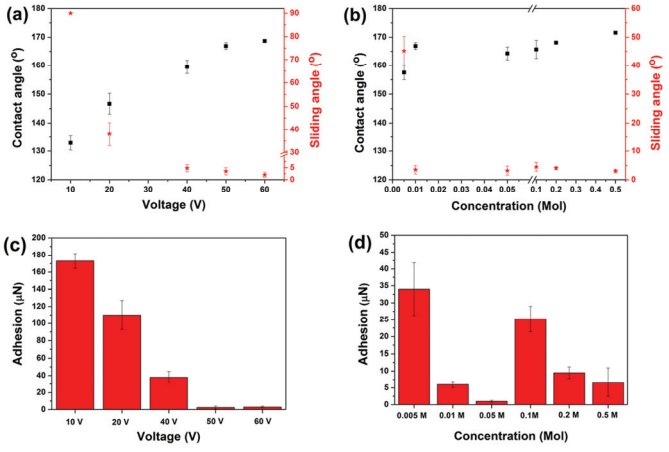

Figure 6. The effect of (a) electrochemical anodizing voltage in 0.01 M NH_4F electrolyte for 1 h, and (b) concentration of NH_4F solution anodized at 50 V for 1 h on static contact angle and dynamic sliding angle of the PDES modified TiO_2 surface. The effect of (c) electrochemical anodizing voltage in 0.01 M NH_4F electrolyte for 1 h, and (d) concentration of NH_4F solution anodized at 50 V for 1 h on droplet adhesion of the PDES modified TiO_2 surface.

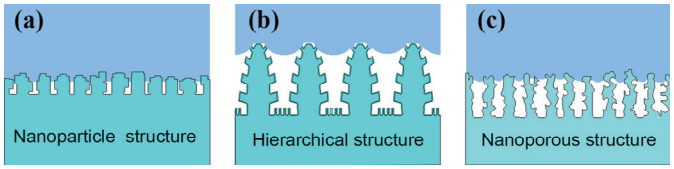

Figure 7. Schematic illustration of three kinds of TiO_2 structures with various liquid-solid contact states and resultant extremely high adhesive forces contrast. a) High-adhesive nanoparticle structure with "Rose" state (a special case of Wenzel's hydrophobic state); b) Low-adhesive hierarchical structure with "Lotus" state (a special case of Cassie's superhydrophobic state); c) Medium-adhesive nanoporous structure with metastable superhydrophobic state between Cassie's and Wenzel's states.

In the previous section, it was shown that the anodized voltage and electrolyte concentration have a strong effect of adhesion contrast for liquid droplets on anti-wetting TiO_2 substrates. The underlying mechanism is that the different topographical morphology induced various liquid-solid contact models to create high contract solid-liquid adhesion.[27,28] We therefore discuss the implementation of the adhesion contrast on some typical micro-droplet manipulation: separation, moving, mixing, transportation and self-assembling (Figure 8, Movie S2,3). Compared to the difficult manipulation of oil droplet (droplet pinning or surface contamination are usually taking place especially for liquid with low surface tension) on conventional hydrophobic substrates, the underwater superoleophobic substrates have a special combination of minimal contact area and insulating water layer to inhibit oil pinning or contamination. Due to the uncontrollable sitting places and easily sliding off on uniform superhydrophobic substrates, it still remains a challenge for facile site and volume controllable self-assembling. Moreover, the patterned super-antiwetting surface is invisible under ambient atmosphere (Fig. 8e). Such wetting patterns can only be visible under some specific conditions, e.g. humid air, dye labelling, or water/oil wetting, These properties make the patterned superhydrophobic substrates to serve as reversible anti-counterfeiting pattern and universal miniature reactor for liquid-liquid/liquid-gas reaction, or even wetting template for site-selective multifunctional nanostructures deposition.[29,30] In a proof-of-concept study, a pink-dyed oil droplet can be totally or partially picked up easily with a needle straw or glass pipette, and re-dropped it on underwater superoleophobic substrate to form two separated droplets. Such two separated droplets can also be mixed together to a bigger droplet without liquid lost.

Water droplets on low-adhesive superhydrophobic substrate with a "Cassie" liquid-solid contact model can be un-loss transported to high-adhesive superhydrophobic substrate with a metastable contact models between Wenzel's and Cassie's states under ambient condition by taking advantage of their high adhesion contrast (Figure. 9a). Similar to the water droplets transportation on substrate with various liquid-solid contact models, liquid with low surface tension on super-wetting surfaces can also be manipulated to contact, attach and collect (Figure 9b, Movie S4,5). For example, oil droplets can be un-loss transported between underwater superoleophobic substrates (superhydrophilic under ambient condition) and released to targeted underwater superoleophilic substrates (superhydrophobic under ambient condition) by taking advantage of the environment responsive contact model change resulted in the wettability and adhesion conversion.

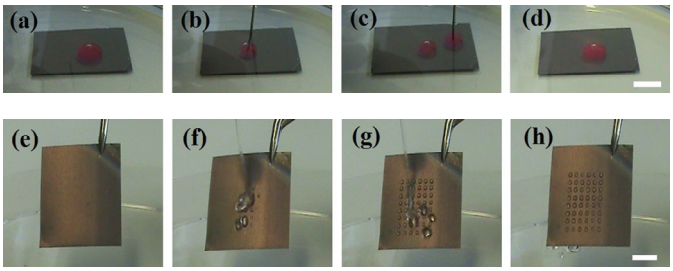

Figure 8. Typical oil droplet (1,2-dichloroethane dyed pink) manipulation based on the underwater superoleophobic substrate. Before (a) and after (b) droplet separation; before (c) and after (d) droplet mixing with the assistance of a syringe. (e-h) Optical image of patterned superhydrophobic TiO_2 surface before (e) and after (f-h) liquid self-assembling. The scale bar is 5 mm.

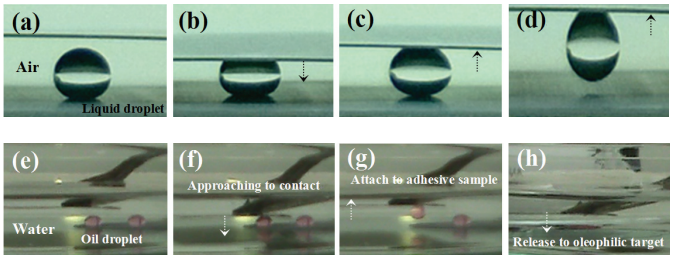

Figure 9. (a-d) Typical liquid droplet transportation process (contact, move and release) based on the extreme high adhesion contrast of the superhydrophobic surface under ambient atmosphere. (e-h) Typical underwater oil droplet dyed pink with 1,2-dichloroethane transportation process by taking advantage of the extreme high adhesion contrast of the underwater superoleophobic surface.

Conclusions

We have successfully developed a rapid and facile one-step electrochemical anodizing process for the creation of hierarchical anatase TiO_2 surface in environmental-friendly electrolyte. The as-prepared TiO_2 surface exhibited superwettability in air or underwater environment, and patterned superhydrophobicity with extremely high wettability and adhesion contrast through the photocatalytic degradation of organic monolayer. The wettability patterns on TiO_2 samples can be quickly removed and regenerated by a novel combination of UV illumination and self-assembling process, and adhesion on superhydrophobic TiO_2 surface can also be controlled between sticky and sliding by regulating the surface morphology (size and density) to control the solid-liquid contact state. Moreover, practical applications of superwettability and patterned superhydrophobic TiO_2 surface in droplet manipulation (separation, mixing, transportation and collection), liquid self-assembly and anti-counterfeiting marks were also demonstrated. The results provide new insights into how to control the wettability and adhesion by adjusting the topographical structure and surface chemistry.

Acknowledgements

The authors thank the Alexander von Humboldt (AvH) Foundation of Germany, Natural Science Foundation of Jiangsu Province of China (No. BK20130313; BK20140400), National Science Foundation of China under Grant 91027039 and 51373110, the Priority Academic Program Development of Jiangsu Higher Education Institutions (PAPD), Project for Jiangsu Scientific and Technological Innovation Team (2013), and Jiangsu Planned Projects for Postdoctoral Research Funds (No. 1302099B) for the financial support of this work.

Notes and references

[a] National Engineering Laboratory of Modern Silk, College of Textile and Clothing Engineering, Soochow University, Suzhou 215123, PR China.
[b]Physikalisches Institute and Center for Nanotechnology (CeNTech), Westfälische Wilhelms-Universität Münster, Münster D-48149, Germany.
[c]School of Materials Science and Engineering, University of Science and Technology Beijing, Beijing100083, PR China.
[d]Institue of Functional Nano & Soft Materials (FUNSOM), Soochow University, Suzhou 215123, PR China.
E-mail: yklai@suda.edu.cn

†Electronic Supplementary Information (ESI) available: [details of any supplementary information available should be included here]. See DOI: 10.1039/b000000x/

1 L. Feng, S. H. Li, Y. S. Li, H. J. Li, L. J. Zhang, J. Zhai, Y. L. Song, B. Q. Liu, L. Jiang and D. B. Zhu, *Adv. Mater.*, 2002, **14**, 1857; M. J. Liu and L. Jiang, *Adv. Funct. Mater.*, 2010, **20**, 3753; c) K. S. Liu, X. Yao and L. Jiang, *Chem. Soc. Rev.*, 2010, **39**, 3240.

2 a) Y. M. Zheng, H. Bao, Z. B. Huang, X. L. Tian, F. Q. Nie, Y. Zhao, J. Zhai and L. Jiang, *Nature*, 2010, **463**, 640; b) K. Autumn, Y. A. Liang, S. T. Hsieh, W. Zesch, W. P. Chan, T. W. Kenny, R. Fearing and R. J. Full, *Nature*, 2000, **405**: 681; c) X. Deng, L. Mammen, H. J. Butt and D. Vollmer, *Science*, 2012, **335**, 67.

3 a) X. Zhang, F. Shi, J. Niu, Y. G. Jiang and Z. Q. Wang, *J. Mater. Chem.*, 2008, **18,** 621; b) Q. D. Xie, J. Xu, L. Feng, L. Jiang, W. H. Tang, X. D. Luo and C. C. Han, *Adv. Mater.*, 2004, **16**, 302; c) X. F. Wu and G. Q. Shi, *J. Phys. Chem. B*, 2006, **110**, 11247.

4 a) W. Barthlott and C. Neinhuis, *Planta*, 1997, 202, 1; b) X. F. Gao and L. Jiang, *Nature*, 2004, **432**, 36; c) X. Q. Feng, X. F. Gao, Z. N. Wu, L. Jiang and Q. S. Zheng, *Langmuir*, 2007, **23**, 4892.

5 a) L. Feng, Y. A. Zhang, J. M. Xi, Y. Zhu, N. Wang, F. Xia and L. Jiang, *Langmuir*, 2008, **24**, 4114; b) B. Bhushan and E. K. Her, *Langmuir*, 2010, **26**, 8207; c) S. Yang, J. Ju, Y. C. Qiu, Y. X. He, X. L. Wang, S. X. Dou, L. S. Liu and L. Jiang, *Small*, 2014, **10**, 294.

6 a) M. J. Liu, S. T. Wang, Z. X. Wei, Y. L. Song and L. Jiang, *Adv. Mater.*, 2009, **21**, 665; b) J. L. Yong, F. Chen, Q. Yang, D. S. Zhang, U. Farooq, G. Q. Du and X. Hou, *J. Mater. Chem. A*, 2014, **2**, 8790; c) L. B. Zhang, Y. J. Zhong, D. Cha and P. Wang, *Sci. Rep.*, 2013, **3**, 2326; d) Q. F. Cheng, M. Z. Li, F. Yang, M. J. Liu, L. Li, S. T. Wang and L. Jiang, *Soft Matter*, 2012, **8**, 6740; e) Q. F. Cheng, M. Z. Li, Y. M. Zheng, B. Su, S. T. Wang and L. Jiang, *Soft Matter*, 2011, **7**, 5948.

7 a) A. R. Parker and C. R. Lawrence, *Nature*, 2001, **414**, 33; b) L. Zhai, M. C. Berg, F. C. Cebeci, Y. Kim, J. M. Milwid, M. F. Rubner and R. E. Cohen, *Nano Lett.*, 2006, **6**, 1213; c) R. Dufour, P. Brunet, M. Harnois, R. Boukherroub, V. Thomy and V. Senez, *Small*, 2012, **23**, 1229.

8 a) X. Deng, L. Mammen, Y. F. Zhao, P. Lellig, K. Mullen, C. Chen, H. J. Butt and D. Vollmer, *Adv. Mater.*, **2**011, **23**, 2962; b) Y. K. Lai, Y. X. Tang, J. J. Gong, D. G. Gong, L. F. Chi, C. J. Lin and Z. Chen, *J. Mater. Chem.*, 2012, **22**, 7420; c) R. Furstner, W. Barthlott, C. Neinhuis and P. Walzel, *Langmuir*, 2005, **21**, 956; d) A. Nakajima, K. Hashimoto, T. Watanabe, K. Takai, G. Yamauchi and A. Fujishima, *Langmuir*, 2000, **16**, 7044.

9 a) Z. G. Guo, W. M. Liu and B. L. Su, *J. Colloid Interface Sci.*, 2011, **353**, 335; b) B. Bhushan and Y. C. Joch, *Langmuir*, 2009, **25**, 3240; c) G. D. Bixler and B. Bhushan, *Nanoscale*, 2014, **6**, 76; d) D. T. Ge, L. L. Yang, Y. F. Zhang, Y. D. Rahmawan and S. Yang, *Part. Part. Syst. Charact.*, 2014, **7**, 763.

10 a) J. Ju, H. Bai, Y. M. Yong, T. Y. Zhao, R. C. Fang, L. Jiang, *Nature Commun.*, **2012**, **3**, 1247; b) D. Wu, S. Z. Wu, Q. D. Chen, Y. L. Zhang, J. Yao, X. Yao, L. G. Niu, J. N. Wang, L. Jiang and H. B. Sun, *Adv. Mater.*, 2011, **23**, 545; c) X. Yao, J. Gao, Y. L. Song and L. Jiang, *Adv. Funct. Mater.*, 2011, **21**, 4270.

11 a) X. J. Liu, Y. M. Liang, F. Zhou and W. M. Liu, *Soft Matter*, 2012, **8**, 2070; b) Y. K. Lai, C. J. Lin, J. Y. Huang, H. F. Zhuang, L. Sun and T. Nguyen, *Langmuir*, 2008, **24**, 3867; c) M. J. Hancock, K. Sekeroglu and M. C. Demirel, *Adv. Funct. Mater.*, 2012, **22**, 2223; d) S. M. Kang, S. Hwang, S. H. Jin, C. H. Choi, J. Kim, B. J. Park, D. Lee and C. S. Lee, *Langmuir*, 2014, **30**, 2828.

12 a) L. Zhai, M. C. Berg, F. C. Cebeci, Y. Kim, J. M. Milwid, M. F. Rubner and R. E. Cohen, *Nano Lett.*, 2006, **6**, 1213; b) Y. K. Lai, Y. X. Tang, J. Y. Huang, F. Pan, Z. Chen, K. Q. Zhang, H. Fuchs and L. F. Chi, *Sci. Rep.*, 2013, **3**, 3009; c) R. Dufour, P. Brunet, M. Harnois, R. Boukherroub, V. Thomy and V. Senez, *Small*, 2012, **23**, 1229.

13 a) M. B. Oliveira, C. L. Salgado, W. L. Song and J. F. Mano, *Small*, 2013, **9**, 768; b) W. L. Song and J. F. Mano, *Soft Matter*, 2013, **9**, 2985; c) E. Ueda and P. A. Levkin, *Adv. Mater.*, 2013, **25**, 1234; d) D. Zahner, J. Abagat, F. Svec, J. M. J. Frechet and P. A. Levkin, *Adv. Mater.*, 2011, **23**, 3030.

14 a) T. S. Wong, S. H. Kang, S. K. Y. Tang, E. J. Smythe, B. D. Hatton, A. Grinthal and J. Aizenberg, *Nature*, 2011, **477**, 443; b) J. Y. Shiu and P. L. Chen, *Adv. Funct. Mater.*, 2007, **17**, 2680; c) T. Ishizaki, N. Saito and O. Takai, *Langmuir*, 2010, **26**, 8147; d) J. Y. Huang, Y. K. Lai, F. Pan, L. Yang, H. Wang, K. Q. Zhang, H. Fuchs and L. F. Chi, *Small*, 2014, Doi:10.1002/smll.201401024.

15 a) F. L. Geyer, E. Ueda, U. Liebel, N. Grau and P. A. Levkin, *Angew. Chem. Int. Edit.*, 2011, **50**, 8424; b) C. F. Jin, Y. F. Jiang, T. Niu and J. G. Huang, *J. Mater. Chem.*, 2012, **22**, 12562; c) A. I. Neto, C. A. Custodio, W. L. Song and J. F. Mano, *Soft Matter*, 2011, **7**, 4147.

16 a) H. Y. Erbil, A. L. Demirel, Y. Avci and O. Mert, *Science*, 2003, **299**, 1377; b) S. T. Wang, L. Feng and L. Jiang, *Adv. Mater.*, 2006, **18**, 767; c) Y. C. Jung and B. Bhushan, *Nanotechnology*, 2006, **17**, 4970; d) J. Li, K. Kreppenhofer, R. Segura, L. Popp, M. Rossi, P. Tzvetkova, B. Luy, C. J. Kähler, A. E. Guber and P. A. Levkin, *Langmuir*, 2013, **29**, 3797.

17 a) J. Yang, Z. Z. Zhang, X. H. Xu, X. T. Zhu, X. H. Men and X. Y. Zhou, *J. Mater. Chem.*, 2012, **22**, 2834; b) X. Y. Zhou, Z. Z. Zhang, X. H. Xu, F. Gao, X. T. Zhu, X. H. Men and B. Ge, *ACS Appl. Mater. Interfaces*, 2013, **5**, 7208; c) G. Hayase, K. Kanamori, M. Fukuchi, H. Kaji and K. Nakanishi, *Angew. Chem., Int. Ed.*, 2013, **52**, 1986; d) K. Nakata, S. Nishimoto, A. Kubo, D. Tryk, T. Ochiai, T. Murakami and A. Fujishima, *Chem. Asian J.*, 2009, **4**, 984.

18 a) J. C. Hulteen and C. R. Martin, *J. Mater. Chem.*, 1997, **7**, 1075; b) D. V. Bavykin, J. M. Friedrich and F. C. Walsh, *Adv. Mater.*, 2006, **18**,

2807; c) X. M. Sun and Y. D. Li, *Chem. Eur. J.*, 2003, **9**, 2229; d) Y. K. Lai, H. F. Zhou, Z. Zhang, Y. X. Tang, Q. L. Tay, J. W. C. Ho, J. Y. Huang, K. Q. Zhang, Z. Chen and B. P. Binks, *Part. Part. Syst. Charact.*, 2014, Doi: 10.1002/ppsc.201400149; e) T. Kasuga, M. Hiramatsu, A. Hoson, T. Sekino and K. Niihara, *Langmuir*, 1998, **14**, 3160.

19 a) C. A. Grimes, *J. Mater. Chem.*, 2007, **17**, 1451; b) P. Roy, S. Berger and P. Schmuki, *Angew. Chem., Int. Ed.*, 2011, **502**, 2904; c) L. N. Wang, L. X. Lin, C. J. Lin, C. Shen, A. Shinbine and J. L. Luo, *J. Nanosci. Nanotech.*, 2013, **13**, 5316; d) J. Wang and Z. Q. Lin, *Chem. Asian J.*, 2012, **7**, 2754; e) M. D. Ye, J. J. Gong, Y. K. Lai, C. J. Lin and Z. Q. Lin, *J. Am. Chem. Soc.*, 2012, **134**, 15720.

20 a) H. Bellanger, T. Darmanin, E. Taffin de Givenchy and F. Guittard, *Chem. Rev.*, 2014, **114**, 2694; b) H. Zhu, Z. G. Guo and W. M. Liu, *Chem. Commun.*, 2014, **50**, 3900; c) D. L. Tian, Y. L. Song and L. Jiang, *Chem. Soc. Rev.*, 2013, **42**, 518; d) X. J. Feng, J. Zhai and L. Jiang, *Angew. Chem., Int. Ed., 2005,* **44**, *5115.*

21 a) D. A. Wang, Y. Liu, X. J. Liu, F. Zhou and W. M. Liu, *Chem. Commun.*, 2009, **45**, 7018; b) W. Sun, S. X. Zhou, B. You and L. M. Wu, *J. Mater. Chem. A*, 2013, **1**, 3146; c) Z. J. Cheng, H. Lai, Y. Du, K. W. Fu, R. Hou, C. Li, N. Q. Zhang and K. N. Sun, *ACS Appl. Mater. Interfaces*, 2014, **6**, 636; d) Y. H. Xiu, L. B. Zhu, D. W. Hess and C. P. Wong, *J. Phys. Chem. C*, 2008, **112**, 11403.

22 a) Y. K. Lai, X. F. Gao, H. F. Zhuang, J. Y. Huang, C. J. Lin and L. Jiang, *Adv. Mater.*, 2009, **21**, 3799; b) Y. K. Lai, L. X. Lin, F. Pan, J. Y. Huang, R. Song, Y. X. Huang, C. J. Lin, H. Fuchs and L. F. Chi, *Small*, 2013, **17**, 2945; c) Y. K. Lai, F. Pan, C. Xu, H. Fuchs and L. F. Chi, *Adv. Mater.*, 2013, **25**, 1682.

23 a) T. Darmanin, E. Taffin de Givenchy, S. Amigoni and F. Guittard, *Adv. Mater.*, 2013, **25**, 1378; b) A. Fujishima, X. T. Zhang and D. A. Tryk, *Surf. Sci. Rep.*, 2008, **63**, 515; c) L. D. Sun, X. Y. Wang, M. L. Li, S. Zhang and Q. Wang, *Langmuir*, 2014, **30**, 2835; d) D. Gong, C. A. Grimes, O. K. Varghese, W. C. Hu, R. S. Singh, Z. Chen and E. C. Dickey, *J. Mater. Res.*, 2001, **16**, 3331

24 a) Y. K. Lai, L. Sun, Y. C. Chen, H. F. Zhuang, C. J. Lin and J. W. Chin, *J. Electrochem. Soc.*, 2006, **153**, D123; b) Y. K. Lai, J. Y. Huang, H. F. Zhuang, V. P. Subramaniam, Y. X. Tang, D. G. Gong, L. Sundar, L. Sun, Z. Chen and C. J. Lin, *J. Hazard. Mater.*, 2010, **184**, 855; c) I. Paramasivam, H. Jha, N. Liu and P. Schmuki, *Small*, 2012, **8**, 3073.

25 a) K. F. Huo, H. R. Wang, X. M. Zhang, Y. Cao and P. K. Chu, *ChemPlusChem*, 2012, **77**, 323; b) Y. L. Liao, W. X. Que, P. Zhong, J. Zhang and Y. C. He, *ACS Appl. Mater. Interfaces*, 2011, **3**, 2800; c) J. Lin, X. L. Liu, M. Guo, W. Lu, G. G. Zhang, L. M. Zhou, X. F. Chen and H. T. Huang, *Nanoscale*, 2012, **4**, 5148.

26 a) N. K. Allam, K. Shankar and C. A. Grimes, *J. Mater. Chem.*, 2008, **18**, 2341; b) Y. X. Tang, Y. K. Lai, D. G. Gong, K. H. Goh, T. T. Lim, Z. L. Dong and Z. Chen, *Chem. Eur. J.*, 2010, **16**, 7704; c) Y. X. Tang, P. X. Wee, Y. K. Lai, X. P. Wang, D. G. Gong, P. D. Kanhere, T. T. Lim, Z. L. Dong and Z. Chen, *J. Phys. Chem. C*, 2012, **116**, 2772.

27 a) A. B. D. Cassie and S. Baxter, *Trans. Faraday Soc.*, 1944, **40**, 546; b) R. N. Wenzel, *Ind. Eng. Chem.*, 1936, **28**, 988.

28 a) A. Tuteja, W. Choi, M. Ma, J. M. Mabry, S. A. Mazzella, G. C. Rutledge, G. H. McKinley and R. E. Cohen, *Science*, 2007, **318**, 1618; b) S. T. Wang, L. Jiang, *Adv. Mater.*, 2007, **19**, 3423; c) W. Xu and C. H. Choi, *Phys. Rev. Lett.*, 2012, **109**, 024504.

29 a) X. L. Liu, J. Gao, Z. X. Xue, L. Chen, L. Lin, L. Jiang and S. T. Wang, *ACS Nano*, 2012, **6**, 5614; b) M. H. Jin, J. Wang, X. Yao, M. Y. Liao, Y. Zhao and L. Jiang, *Adv. Mater.*, 2011, **23**, 2861; c) B. Su, S. T. Wang, Y. L. Song and L. Jiang, *Soft Matter*, 2011, **7**, 5144; d) X. Chen, Y. C. Wu, B. Su, J. M. Wang, Y. L. Song and L. Jiang, *Adv. Mater.*, 2012, **24**, 5884.

30 a) A. K. Kota, Y. X. Li, J. M. Mabry and A. Tuteja, *Adv. Mater.*, 2012, **24**, 5838; b) Z. X. Xue, S. T. Wang, L. Lin, L. Chen, M. J. Liu, L. Feng and L. Jiang, *Adv. Mater.*, 2011, **23**, 4270; c) N. Tretyakov and M. Muller, *Soft Matter*, 2014, **10**, 4373.

Graphical Abstract:

Adhesive forces on superhydrophobic nanostructure surface may be tailored with an extremely high contrast (2.5-170 μN) by modifying structural morphology to manipulate solid-liquid contact state.